

FLAME HEAT FLUXES IN PMMA POOL FIRES

Naeem Iqbal* and James Quintiere
Department of Fire Protection Engineering
College of Engineering
University of Maryland
College Park, Maryland 20742-3031, USA

SUMMARY

A simple one-dimensional analytical model has been developed to describe the processes involved in the transient burning of non-charring thermoplastic materials. The model includes conduction, convection, and radiation effects for flaming materials. The burning rate solution is obtained by numerically solving an ordinary differential equation and an algebraic equation with flame radiative heat flux as a specified variable. The effect of convective blowing is also included in the model. The model is used to compute the flame heat fluxes for PMMA pool fires at various sizes. The results show the range of convective and radiative heat fluxes from the PMMA flame for pool fires ranging from 0.023 to 1.50 m² or 0.151 - 1.22 m diameter.

INTRODUCTION

A fire typically starts from ignition of solid or liquid fuels. Solid and liquid fuels serve as suppliers of gaseous fuel in support of fire. This mass loss, or burning rate, is governed by the heat transfer at the surface of the fuel. In general, the burning of a solid is not a steady state phenomena, but is a complex process involving gas phase reactions, conduction, convection, and radiation heat transfer, diffusion of gaseous species, and chemical decomposition of the condensed phase fuel. The dynamic burning of solid materials is one of the key and difficult topics to be addressed in the evaluation of material flammability and fire safety. The way a building fire develops and spreads, and the amount of damage that ensues, is greatly influenced by the characteristics of the burning due to interior furnishings and contents. Therefore, in order to ensure life and building fire

safety it is important to be able to predict the transient burning rate of solid materials. In view of the complexity of the burning process, a general model for the prediction of the burning rate of a solid is not available. Specific models have been developed, but they are limited to specific classes of materials and do not apply in general. Consequently, the evaluation of materials and products for contribution to fire has been subject to interpretation and empirical practices.

A principal factor that affects the dynamic burning of a solid material is the flame heat flux. The heat flux received from the flame controls the burning behavior of the solid or liquid fuel. A knowledge of flame heat flux is also important in the interpretation of material test data and its relationship to real fire scenarios. Models for burning rate and flame spread require such heat flux information. In particular, the flame radiative heat flux is the least understood, yet it is the dominant flux in

* Current address is Hughes Associates, Inc., 6770 Oak Hall Lane, Suite 125, Columbia, Maryland 21045.

realistic fires. Despite this need, it is surprising that so little is known about the flame heat flux under realistic fire conditions. The effects of scale, orientation, and enclosure have not been studied in a systematic way. Lacking fundamental approaches that can be practically implemented, it is suggested that experimental correlations might have greater immediate practicality. However, data are lacking to even explore such an approach. In this study, flame heat flux will be computed from the burning rate data of PMMA pool fires. These results should also apply to other fuels of similar radiative properties.

Recently Iqbal¹ has presented a one-dimensional analytical burning rate model to describe the processes involved in the dynamic burning of a solid thermoplastic material. The burning rate model includes flame and external radiation, conduction, and convection effects. The burning rate solution is obtained by numerically solving an ordinary differential equation and an algebraic equation. It considers an integral approach to the burning rate of a finite solid. Flame radiation heat flux must be specified, and can be a function of mass loss rate. The gas phase aspects are considered steady, whereas the solid phase is one-dimensional and unsteady.

A non-flaming analysis has been described by Quintiere and Iqbal². A similar analysis has also been present by Agrawal and Atreya³. These show good accuracy of the approximate integral solution with exact numerical and experimental results of PMMA. Hence, applications to PMMA are expected to yield good results. Other burning rate models for thermoplastic are also available. Steckler *et. al.*⁴ have presented a one-dimensional analytical model for transient gasification of non-charring materials similar to Quintiere and Iqbal² using a different approximate analytical method. Delichatsios and Chen⁵ have provided a numerical solution for pyrolysis of non-charring materials. Vovella *et. al.*⁶ have conducted a theoretical and experimental investigation of the thermal degradation of PMMA.

Their theoretical results are in good agreement with measured mass loss rates and measured temperature distribution in the vaporizing PMMA. Kindelan and Williams⁷ used asymptotic expansions to obtain a solution to a semi-infinite solid undergoing pyrolysis subject to a constant heat flux. These models all vary in their degree of approximations. Some include pyrolysis kinetics for a decomposition model in contrast to the simple constant temperature surface evaporation used here. Generally, it is found that the surface evaporation model is valid for high enough heat fluxes which are expected in this application of flame heat transfer.

Modak and Croce⁸ have investigated burning behavior of horizontal PMMA pools (PMMA [polymethylmethacrylate], a plastic known commercially as plexiglas was chosen because of its ideal representation as a thermoplastic, and its widespread use in research) of varying sizes. The pool fire configuration includes flame radiative and convective effects, transient heat conduction, laminar and turbulent burning. They investigated the burning rate of 51 mm thick horizontal PMMA pool fires. This study yielded excellent data on the transient burning rate of square pools ranging in size from 0.023 m² to 1.5 m², or 15 cm to 1.22 m on a side. These sizes are expected to produce laminar to turbulent burning conditions as size increases. Surface heat fluxes were not measured in their study, but Modak and Croce inferred the flame radiative heat flux by using the measured mass loss rate in a one-dimensional transient pyrolysis model of the PMMA. In their analysis, they assumed a constant flame convective heat flux of 6.4 kW/m² which does not account for any variations due to surface blowing effects. However, a significant error was introduced when they did not include the effect of surface re-radiation. They used a numerical model to perform this analysis. Because of this error, it was decided to recompute these flame heat fluxes with the approximate burning rate model developed by Quintiere and Iqbal². In doing so, we included the effect

of blowing by the stagnant film $\ln(1+ B)$ formulation for convection. Also we corrected their analysis by including the re-radiation term.

Orloff and De Ris⁹ have presented an algorithm for the burning of moderate scale (0.1-0.7 m diameter) PMMA pool fires in terms of the pool scale and fuel properties. They developed an empirical equation for flame radiation as a function of the burning rate. Under some conditions, when flame radiation is underpredicted, a solution for burning rate is not possible. Our attempts at incorporating their formula led to such results. Brosmer and Tien¹⁰ have presented a model for flame radiation and fuel radiative blockage in PMMA pool fires. Their model included an inner cone of fuel within a homogeneous flame zone. Their results were compared to the steady state heat flux results computed by Modak and Croce⁸. We shall show the corrected results and this new comparison later.

MATHEMATICAL FORMULATION AND DERIVATION

The present burning rate model is an extension of the purely pyrolysis non-flaming model of semi-infinite thermoplastic material under external radiative heat flux presented by Quintiere and Iqbal². An example

of the results is shown in Figures 1 and 2, where the preheating temperature is shown before ignition occurs. Also a physical description of the thermoplastic model is shown in Figure 3. Since this solution has good accuracy when tested against numerical results, it was decided to apply it to the data of Modak and Croce⁸.

The model for a semi-infinite thermoplastic material, includes preheating to ignition before pyrolysis based on the use of ignition temperature. Also, only surface vaporization is considered at a constant vaporization temperature. An integral solution

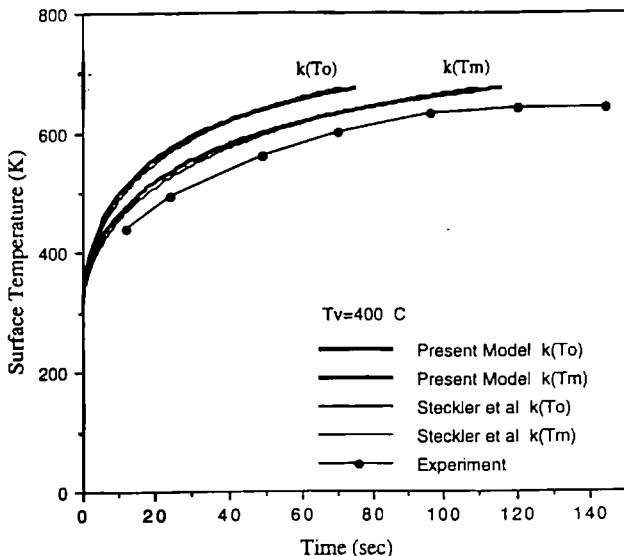


Figure 1. Surface temperature of PMMA exposed to 40 kW/m² incident heat flux.

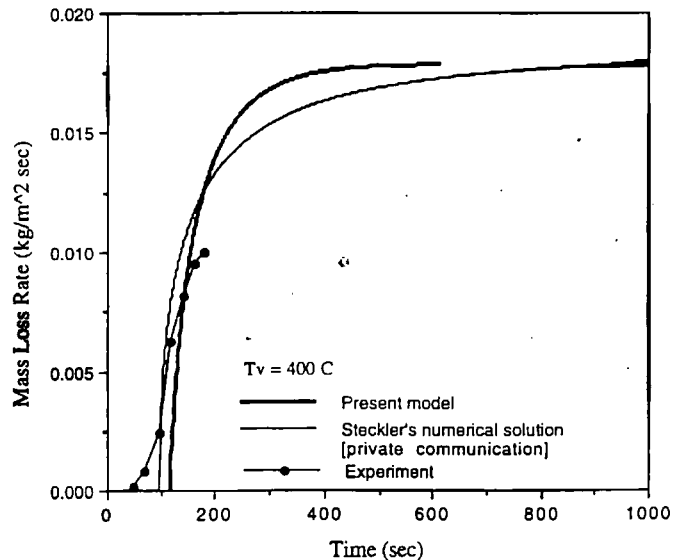


Figure 2. Mass loss rate of PMMA exposed to 40 kW/m² incident heat flux.

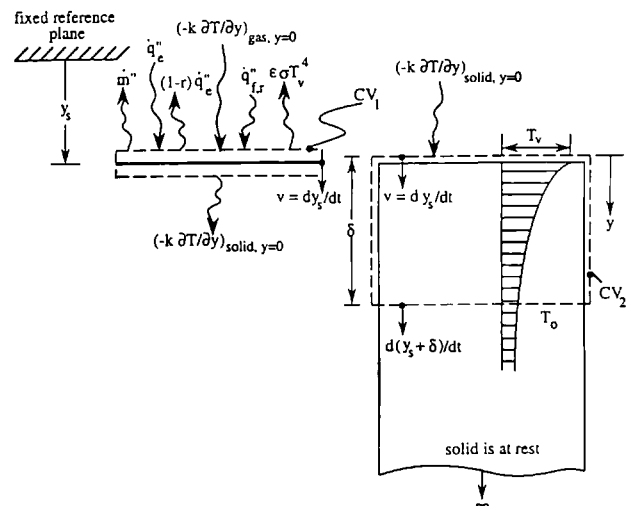


Figure 3. Model for a thermoplastic-like solid material.

yields a solution for the preheating period in terms of a single nonlinear algebraic equation for the net surface heat flux. An extension of the integral solution to the vaporization period yields the following equations for solution.

An energy conservation applied to the control volume for the solid in Figure 4 yields

$$\rho c \frac{d}{dt} \int_0^\delta (T - T_o) dy + \dot{m}'' c (T_v - T_o) = \left(-k \frac{\partial T}{\partial y} \right)_{y=0} \quad (1)$$

where

T - temperature

T_o - ambient temperature

T_v - vaporization temperature

ρ - density of the solid

c - gas phase specific heat

k - thermal conductivity of the solid

\dot{m}'' - mass loss rate per unit area

y - measured downward from the surface

A quadratic profile for temperature is assumed as

$$\frac{T - T_o}{T_v - T_o} = \left(1 - \frac{y}{\delta} \right)^2 \quad (2)$$

which satisfies T_v at the surface and T_o at δ along with zero heat loss. Substituting Equation 2 into Equation 1 yields

$$\frac{1}{3} \frac{d\delta}{dt} + \frac{\dot{m}''}{\rho} = \frac{2\alpha}{\delta} \quad (3)$$

where $\alpha = \frac{k}{\rho c}$ thermal diffusivity of the solid.

A conservation of energy applied to the vaporizing surface control volume in Figure 3 yields

$$\dot{m}'' \Delta H_v = \left(k \frac{\partial T}{\partial y} \right)_{\text{gas}, y=0} + (1 - r_s) (\dot{q}_{f,r}'' + \dot{q}_{ext,r}'') - \varepsilon \sigma T_v^4 - \left(-k \frac{\partial T}{\partial y} \right)_{y=0} \quad (4)$$

$$\left[\begin{array}{l} \text{Rate of energy} \\ \text{to vaporize} \end{array} \right] = \left[\begin{array}{l} \text{Rate of flame} \\ \text{convection} \end{array} \right] + \left[\begin{array}{l} \text{Rate of flame} \\ \text{radiation} \end{array} \right] + \left[\begin{array}{l} \text{Rate of external} \\ \text{radiation} \end{array} \right] - \left[\begin{array}{l} \text{Re-radiation} \\ \text{solid} \end{array} \right] - \left[\begin{array}{l} \text{Conduction into} \\ \text{solid} \end{array} \right]$$

where

$$\left(k \frac{\partial T}{\partial y} \right)_{\text{gas}, y=0} - \text{convective flame heat flux}$$

$\dot{q}_{f,r}''$ - flame radiative heat flux

$\dot{q}_{ext,r}''$ - external radiative heat flux

ε - emissivity of the solid surface

r_s - reflectivity of the solid surface

Equation 4 supplies the thermal boundary condition for the stagnant film model to describe the gas phase reaction zone, based on Kanury¹¹. Specifically this is rewritten as

$$\left(k \frac{\partial T}{\partial y} \right)_{\text{gas}, y=0} = \dot{m}'' \left[\Delta H_v - \frac{1}{\dot{m}''} \left((1 - r_s) (\dot{q}_{f,r}'' + \dot{q}_{ext,r}'' - \varepsilon \sigma T_v^4 - \frac{2k}{\delta} (T_v - T_o)) \right) \right] \quad (5a)$$

$$\left(k \frac{\partial T}{\partial y} \right)_{\text{gas}, y=0} = \dot{m}'' \hat{L} \quad (5b)$$

where the last term comes from substituting Equation 2 into Equation 4, and \hat{L} is defined as an effective heat of gasification which includes transient and radiatives effects.

From Kanury¹¹ it is shown, when Equation 5b is used in place of the steady state pure convective conditions,

$$\dot{m}'' = \frac{h_c}{c_g} \ln(1 + B) \quad (6)$$

where

$$B = \frac{Y_{ox, \infty} (1 - \chi_r) \frac{\Delta H_c}{r} + c_g (T_o - T_v)}{\hat{L}} \quad (7)$$

and

B - Spalding number,
 $Y_{ox, \infty}$ - ambient oxygen mass fraction,
 χ_r - flame radiative fraction,
 r - stoichiometric oxygen to fuel mass ratio, and
 c_g - gas phase specific heat at constant pressure.

Substituting Equation 5 and Equation 7 in Equation 6 gives governing equation for the burning rate

$$\dot{m}'' = \frac{\frac{h_c \left(\frac{\xi}{e^{\xi} - 1} \right) \left[Y_{ox, \infty} (1 - \chi_r) \frac{\Delta H_c}{r} - c_g (T_v - T_o) \right]}{\Delta H_v} - \frac{2k(T_v - T_o) + \dot{q}_{f,r}'' (1 - r_s) - \epsilon \sigma T_v^4}{\delta}} \quad (8)$$

where $\xi = \frac{\dot{m}'' c_g}{h_c}$.

The quantity $\left(\frac{\xi}{e^{\xi} - 1} \right)$ is called the blocking factor, which effectively reduces the heat transfer coefficient h_c from its pure heat transfer value as the mass transfer \dot{m}'' increases.

The algebraic Equation 8 and the first order ordinary differential Equation 3 can be solved simultaneously by an iterative procedure at each time step to obtain consistent convergence.

SOLUTION METHODOLOGY

The burning rate equation requires an initial condition over the thermal penetration depth δ at time of ignition t_i . This is approximated from the preheating integral used by Quintiere and Iqbal², as

$$\delta = \sqrt{6 \alpha t_i} \quad (9)$$

The samples of PMMA in the experiments conducted by Modak and Croce⁸ were ignited by a liquid fuel in the times listed in Table 1. The initial value for δ was computed from Equation 9 at these times.

An application of the present model is now used to compute the flame heat fluxes by using the experimental burning rate data of Modak and Croce⁸. Their results are shown in Figure 4. They were able to represent their experimental results after ignition by the following empirical relation:

$$\frac{\dot{m}_s'' - \dot{m}_i''}{\dot{m}_s'' - \dot{m}_i''} = e^{-t/\theta} \quad (10)$$

The initial burning rate \dot{m}_i'' was taken as 4 g/m² sec. The time constant, θ , and the steady state burning rate \dot{m}_s'' are given in Table 1. In some cases the experimental results did not actually achieve steady state so \dot{m}_s'' is an inferred value.

Pool Area (m ²)	Time After Ignition (s)	Gasification Time θ (s)	Modak and Croce ⁸		Computed Results		
			Measured \dot{m}_s'' ($\frac{g}{m^2 \cdot s}$)	$\dot{q}_{f,r}''$ ($\frac{kW}{m^2}$)	h_c ($\frac{W}{m^2 \cdot K}$)	$\dot{q}_{f,c}''$ ($\frac{kW}{m^2}$)	$\dot{q}_{f,r}''$ ($\frac{kW}{m^2}$)
0.023	250	3448	7.7	6.0	8.3	9.01	12.8
0.052	240	1587	9.0	8.1	7.5	7.01	17.2
0.093	225	2222	15.5	18.5	7.0	3.39	32.0
0.21	188	1136	17.4	21.6	8.1	4.08	34.5
0.37	160	500	18.0	22.6	8.1	3.88	35.7
0.58	150	357	18.30	23.0	8.1	3.80	36.2
1.50	125	118	20.0	25.8	8.1	3.23	39.7

Table 1. Experimental results from Modak and Croce⁸ and computed steady state flame heat fluxes.

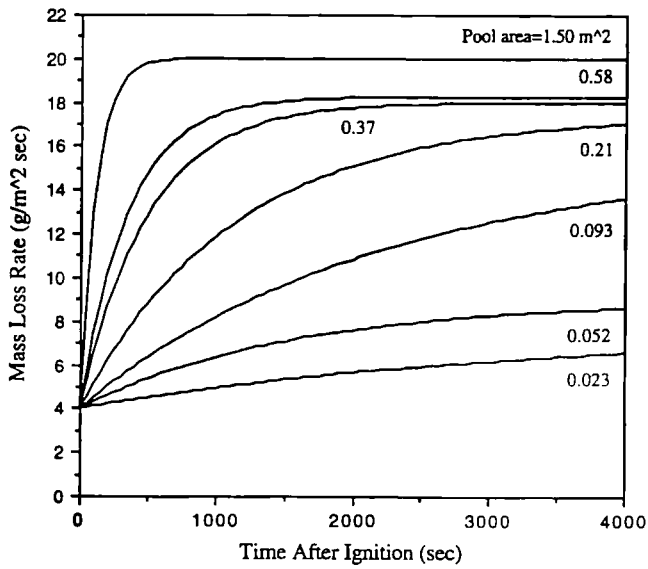


Figure 4. Experimental burning rate for seven square PMMA pool fires⁹.

The flame heat flux can be computed by substituting Equation 10 into Equation 3 and solving for δ by a Runge-Kutta method. Then from Equation 8 and 10, the flame radiative heat flux is computed for each time. The convective heat flux follows from the Equation 8 as

(11)

$$\dot{q}_{f,c}'' = \frac{h_c}{c_g} \left(\frac{\xi}{e^{\xi} - 1} \right) \left[Y_{Ox, \infty} (1 - \chi_r) \frac{\Delta H_c}{\Gamma} - c_g (T_v - T_o) \right]$$

Values selected for the properties and ambient conditions are given in Nomenclature.

The convective heat transfer coefficient was evaluated for natural convection for a horizontal slab face up at a uniform temperature for different pool diameters. From Holman¹².

$$h_c = \frac{k_f}{D} C (Gr_f Pr_f)^m \quad (12)$$

where k_f is the gas phase thermal conductivity at the film temperature T_f , C and m are constants, depends upon type of flow (laminar or turbulent) and the equivalent diameter of the pool:

$$\begin{aligned} (10^5 < Gr.Pr < 2 \times 10^7) & \quad 0.54 (Gr.P)^{1/4} & \text{laminar} \\ (2 \times 10^7 < Gr.Pr < 2 \times 10^{10}) & \quad 0.14 (Gr.P)^{1/3} & \text{turbulent} \end{aligned}$$

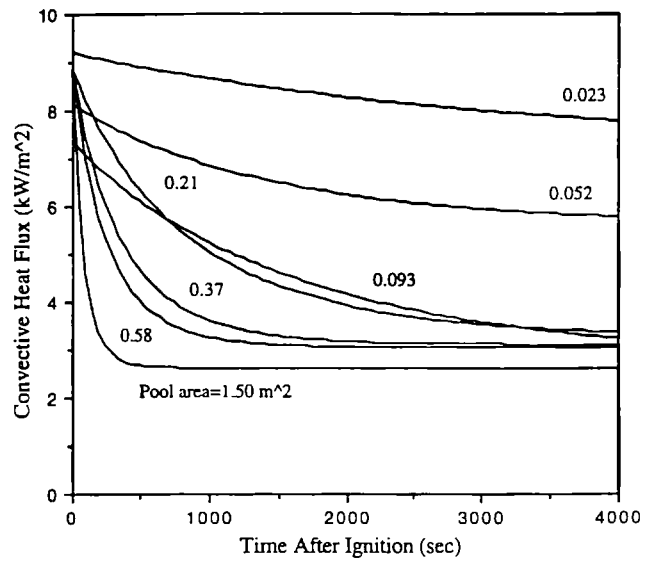


Figure 5. Computed flame convective heat flux for seven square PMMA pool fires.

The calculated values of convective heat transfer coefficient are given in Table 1 for different pool sizes.

RESULTS

The transient convective heat transfer behavior of the different scale pool fires is shown in Figure 5. The convective heat fluxes for large pools drop off rapidly in time, and is significant for earlier time. It suggests that the three smallest pools are laminar, and the rest are turbulent. For large turbulent pool fires the effect of convection heat transfer is much less significant.

Figure 6 shows the computed results of the transient flame radiative heat fluxes for seven different sizes of PMMA pools. These results suggest that the flame radiation is generally higher in large diameter pool fires and is much less significant in small diameter pool fires. It is interesting to note that for the inferred results, the model yields initial results for flame convective heat fluxes of approximately 7.0 to 9.0 kW/m², and the radiative heat fluxes of approximately 15.0 to 20.0 kW/m². As burning increases, the convective heat fluxes decreases to as low as 3.0 kW/m², and the radiative heat flux increases to as high as 40.0 kW/m², for the large pool at steady burning.

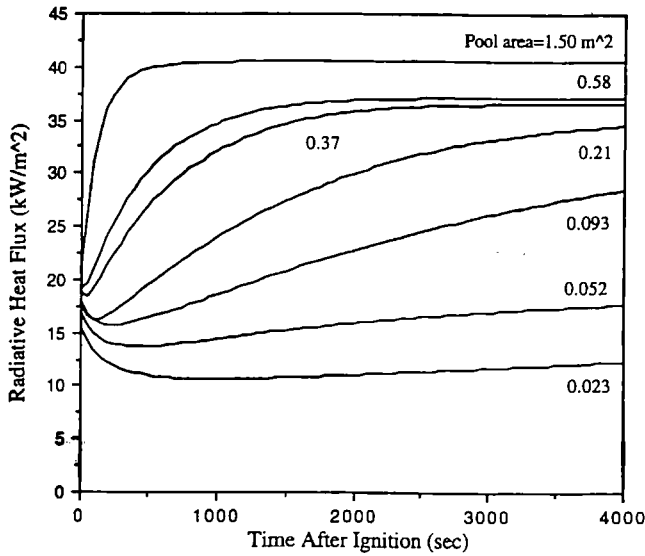


Figure 6. Computed flame radiative heat flux for seven square PMMA pool fires.

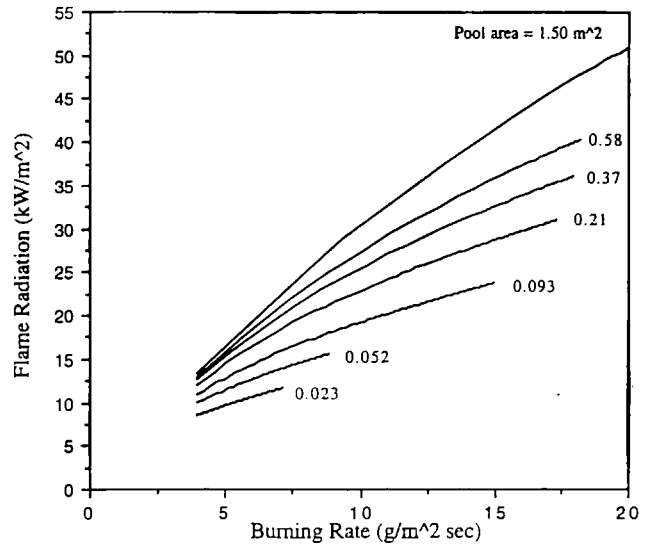


Figure 7. Experimental burning rate for seven square PMMA pool fires vs. Orloff and De Ris⁹ flame radiation model.

Figure 7 shows the results of experimental burning rate data plotted against the flame radiative heat flux computed from the empirical flame radiation equation of Orloff and De Ris⁹.

Figure 8 compares the computed results of laminar and turbulent pool fires. For small pool size (0.023 m²) the flame radiation starts from 15.50 kW/m² and after 4000 seconds drops to 12.30 kW/m². Similarly flame convection starts from 9.0 kW/m² and after 4000 seconds it drops to about 7.80 kW/m². For large pool size (1.50 m²),

flame radiation starts from 20 kW/m² and after 4000 seconds it reaches about 40.50 kW/m². This shows that the flame radiation effects on the burning behavior are significant in turbulent pool fires. The flame convection effects in turbulent pool fires are also significant; flame convective heat flux varies with time from 8.85 kW/m² to 2.6 kW/m². This shows that the blocking effects of the convection in transient burning is initially low and when the fire gets bigger the convection drops because the blocking effects increase at high mass transfer.

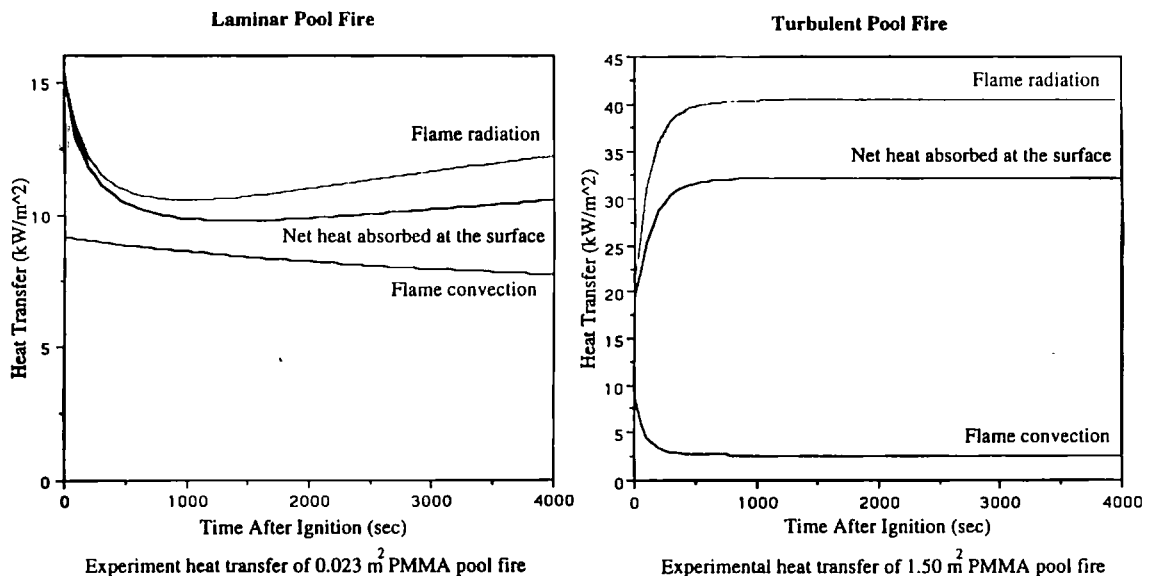


Figure 8. Comparison of experimental flame heat transfer results of 0.023 m² and 1.50 m² PMMA pool fires.

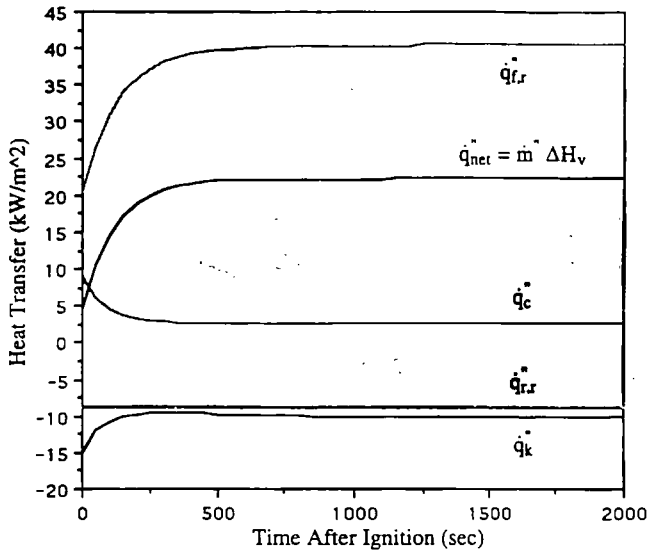


Figure 9. Heat transfer components for a turbulent pool fire 1.50 m² PMMA.

Figure 9 shows heat transfer components for a turbulent pool fire (1.50 m² PMMA). These computations include conduction, re-radiation, convection, fuel gasification (burning rate) and flame radiation.

Figure 10 compares the flame radiation results computed from the present model and the empirical flame radiation prediction of Orloff and De Ris⁹ as a function of the burning rate. Where the prediction of the Orloff and De Ris⁹ model falls below the computed experimental value in Figure 10, the transient burning rate model given by Equations 3 and 8 has no solution. Here the net

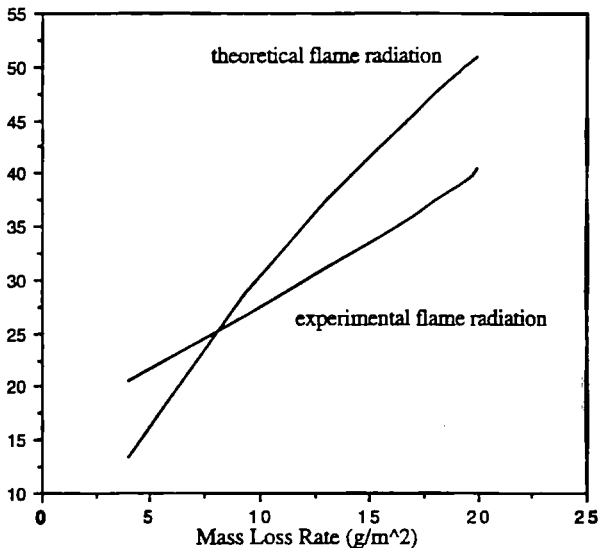


Figure 10. Experimental and theoretical flame radiative heat flux vs. mass loss rate of turbulent pool fire, 1.50 m² PMMA.

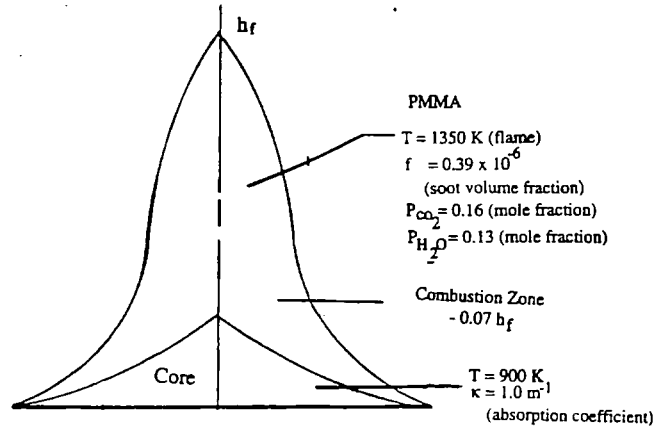


Figure 11. Radiative energy blockage in large pool fires, from Brosmer and Tien¹⁰.

surface heat flux is negative. This shows the sensitivity of the model to flame radiation. Hence, their model could not be used to predict results.

Figure 11 shows a two-region flame shape near the fuel surface developed by Brosmer and Tien¹⁰ for the prediction of flame radiation to the fuel surface for PMMA pool fires. It consists of two homogeneous regions representing combustion and fuel vapor zone. The flame temperatures for combustion and fuel vapor zone are taken as 1350 K and 900 K respectively.

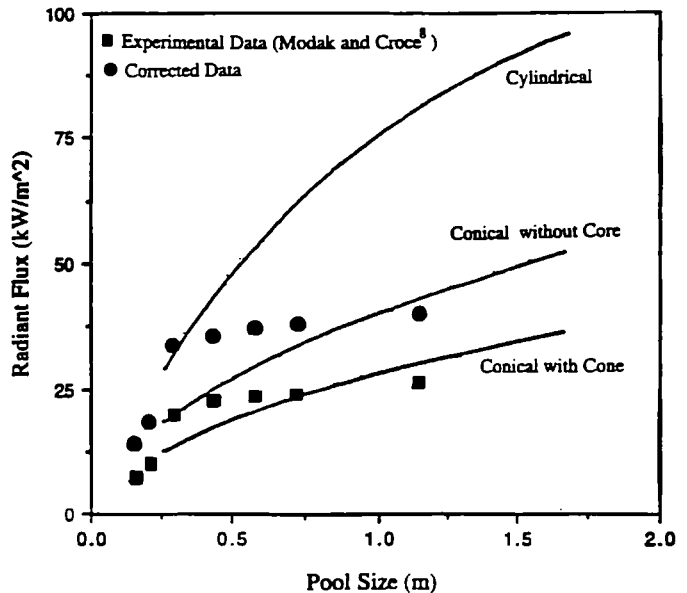


Figure 12. Corrected results of steady flame radiation to pool surface.

Figure 12 shows their results for PMMA pool fires for the conical core vapor zone model, a conical-homogeneous flame model without the vapor zone, and a cylindrical flame model. The experimental results for flame radiation from Modak and Croce⁸ have been corrected in this figure. The corrected results were calculated by including reradiation term, and as described previously.

CONCLUSIONS

A simple approximate burning rate model has been presented to predict the mass loss rate, flame convective and radiative heat transfer for PMMA pool fires. The analytical model is applicable to thermo-plastic materials and can be applied to zone fire models to predict growth of fire in a compartment.

Dynamic results for the flame radiative heat flux in Figure 6 show, as expected, that the flame radiative heat flux will generally increase as the burning rate increases especially for the larger pools. Accurate and complete methods to predict the flame radiation in attempts at predicting the burning rate of real materials have some deficiencies. The approximate model used to infer the flame heat flux for these PMMA pool fires is sufficiently accurate to expect that the inferred results are reasonably reliable.

The radiative models suggested by Orloff and De Ris⁹, and by Brosmer and Tien¹⁰ do not fully explain the observations for flame radiation. Moreover, theoretical solution closure was found to be sensitive to the values of flame radiative heat flux computed. Hence, no general theoretical result for burning rate could be computed.

NOMENCLATURE

The properties are given for PMMA

B - Spalding number

c_g - gas phase specific heat, $1.0 \frac{\text{kJ}}{\text{kg-K}}$

D - equivalent diameter of the square pool

Gr - Grashof number, Equation 12

h_c - convective heat transfer coefficient relevant to the flame system

k - thermal conductivity of solid, $0.209 \times 10^{-3} \frac{\text{kW}}{\text{m-k}}$

\hat{L} - apparent heat of gasification, Equation 5b & 7

\dot{m}'' - mass loss rate per unit area, $\frac{\text{kg}}{\text{m}^2\text{-sec}}$

Pr - Prandtl number, Equation 12

\dot{q}'' - net heat flux, $\frac{\text{kW}}{\text{m}^2}$

$\dot{q}_{f,c}''$ - flame convective heat flux, $\frac{\text{kW}}{\text{m}^2}$

$\dot{q}_{\text{ext},r}''$ - external radiative heat flux.

(Taken as zero in this application)

$\dot{q}_{f,r}''$ - flame radiative heat flux, $\frac{\text{kW}}{\text{m}^2}$

r - effective stoichiometric oxygen to fuel mass ratio, 2.0

r_s - reflectivity of the solid surface, 0.05

t - time, sec

T_o - ambient and initial temperature, 20 °C

T_v - vaporization temperature of the solid, 363 °C

y - space coordinate

$Y_{\text{Ox}, \infty}$ - ambient mass fraction of oxygen, 0.233

α - thermal diffusivity of the solid, $1.2 \times 10^{-7} \frac{\text{m}^2}{\text{sec}}$

σ - Stefan Boltzmann constant, $5.669 \times 10^{-11} \frac{\text{kW}}{\text{m}^2\text{-K}^4}$

ϵ - emissivity of the solid surface, 0.95

ρ - density of the solid, $1190 \frac{\text{kg}}{\text{m}^3}$

δ - thermal penetration depth, m

ΔH_c - effective heat of combustion of the solid,

$$26,000 \frac{\text{kJ}}{\text{kg}}$$

ΔH_v - effective heat of vaporization of the solid,

$$1108 \frac{\text{kJ}}{\text{kg}}$$

θ - gasification time

χ_r - fraction of energy radiated by the flame, 0.42

ξ - blocking factor

REFERENCES

1. Iqbal, N., "Burning Rate Model for Thermoplastic Materials," Master of Science Thesis, Department of Fire Protection Engineering, University of Maryland, College Park, MD, 1993.
2. Quintiere, J. G. and Iqbal, N., "An Approximate Integral Model for the Burning Rate of a Thermoplastic-like Material," *Fire and Materials*, Vol. 18, No. 2, 1994, pp. 89-98.
3. Agrawal, S. and Atreya, A., "Wind-Aided Flame Spread Over an Unsteadily Vaporizing Solid," *Proceedings of the 24th International Symposium on Combustion*, The Combustion Institute, Pittsburgh, PA, 1992, pp. 1693-1685.
4. Steckler, K. D., Kashiwagi, T., Baum, H. R., and Kanemara, K., "Analytical Model for Transient Gasification of Non-Charring Thermoplastic Material," *Proceedings of the 3rd International Symposium on Fire Safety Science*, Elsevier Applied Science, London, 1991, pp. 895-904.
5. Delichatsios, M. A., and Chen, Y., "Asymptotic, Approximate, and Numerical Solution for the Heatup and Pyrolysis of Materials Including Re-radiation Losses," *Combustion and Flame*, Vol. 92, 1993, pp. 292-307.
6. Vovelle, C., Delfau, J-L., Reuillon, R., Bransier, J., and Laraqui, N., "Experimental and Numerical Study of the Thermal Degradation of PMMA," *Combustion Science and Technology*, Vol. 53, 1987, pp. 187-201.
7. Kindelan, M. and Williams, F. A., "Theory for Endothermic Gasification of a Solid by a Constant Energy Flux," *Combustion Science and Technology*, Vol. 10, 1975, pp. 1-9.
8. Modak, A. and Croce, P., "Plastic Pool Fires," *Combustion and Flames*, Vol. 30, 1977, pp. 251-265.
9. Orloff, L. and De Ris, J., "Froude Modeling of Pool Fires," *Proceedings of the 19th International Symposium on Combustion*, The Combustion Institute, Pittsburgh, PA, 1982, pp. 885-895.
10. Brosmer, M.A. and Tien, C. L., "Radiative Blockage in Large Pool Fires," *Combustion Science and Technology*, Vol. 51, 1987, pp. 21-37.
11. Kanury, A. M., *Introduction to Combustion Phenomena*, Gordon and Breach Science Publishers, New York, 1975, pp. 148-172.
12. Holman, J. P., *Heat Transfer*, 7th ed., McGraw-Hill Book Publishing Company, New York 1990, pp. 343.